

# Emissions of fragments and mesons produced in heavy-ion collisions at CSR and related energies<sup>\*</sup>

LIU Fu-Hu(刘福虎)<sup>1,1)</sup> SUN Yan(孙彦)<sup>2</sup> DUAN Mai-Ying(段麦英)<sup>1</sup> LI Jun-Sheng(李俊生)<sup>1</sup>

<sup>1</sup> (Institute of Theoretical Physics, Shanxi University, Taiyuan 030006, China)

<sup>2</sup> (Department of Physics, Shanxi Datong University, Datong 037009, China)

**Abstract** Using a multisource ideal gas (MSIG) model, we reconstruct the transverse emission source in the momentum space for light fragments produced in reactions  $^{86}\text{Kr}-^{124}\text{Sn}$  at 25 MeV/nucleon and  $b=7-10$  fm based on the theoretical predictions of the Isospin-Dependent Quantum Molecular Dynamics (IDQMD) model. We show that the MSIG model can reasonably describe the IDQMD-predicted results for the azimuthal distribution and the transverse momentum dependence of elliptic flow  $v_2$  and fourth-order anisotropic flow  $v_4$  but can only qualitatively describe the transverse momentum spectra. The azimuthal distributions of nuclear fragments produced in heavy-ion collisions at intermediate energies are studied by the MSIG model. The calculated results are compared and found to be in agreement with the experimental data of Ca-Ca, Nb-Nb, and Au-Au collisions at 150–800 MeV/nucleon beam energies. Meanwhile, the angular distributions of pions and kaons produced in heavy-ion collisions at the low-energy end (1–2 GeV/nucleon) of high energies are investigated by the MSIG model, too. The calculated results are compared and found to be in agreement with the experimental data of the KaoS Collaboration.

**Key words** CSR and related energies, heavy-ion collisions, fragment, meson, multisource ideal gas model

**PACS** 25.70.Mn, 25.70.Pq, 25.75.Ld

## 1 Introduction

In the past 20–30 years, the investigations of heavy ion collisions at intermediate and high energies have been progressed rapidly<sup>[1]</sup>. The accelerator Bevalac at the Lawrence Berkeley National Laboratory (LBNL) in USA and the alternating-gradient synchrotron (AGS) at the Brookhaven National Laboratory (BNL) in USA have been built. The Joint Institute for Nuclear Research (JINR) in former the Soviet Union has built the superconducting synchrotron for nuclei and heavy ions (Nuclotron). The Gesellschaft für Schwerionenforschung mbH (GSI) in Germany has built the heavy ion synchrotron (SIS). The fixed target experiments induced by heavy ions have been performing successfully over an energy range from

1 GeV/nucleon to more than 10 GeV/nucleon. The European Organization for Nuclear Research (the European Laboratory of Particle Physics, CERN) in Switzerland has built the Super Proton Synchrotron (SPS). The beam energies have been extended to a few decades and 200 GeV/nucleon. Since June 2000, the Relativistic Heavy Ion Collider (RHIC) has been performing successfully at BNL. The center-of-mass energy of the interacting system reached a few decades to 200 GeV/nucleon<sup>[2, 3]</sup>. It is expected that the Large Hadron Collider (LHC) will be built at CERN soon<sup>[4]</sup>.

The working energies of Bevalac and SIS are at the low-energy end (1–2 GeV/nucleon) of high energies, and those of Nuclotron, AGS, SPS, and RHIC are at the intermediate- and high-stage of high en-

Received 8 July 2008

<sup>\*</sup> Supported by National Natural Science Foundation of China (10675077) and Natural Science Foundation of Shanxi Province (2007011005, 20051002)

1) E-mail: fuhuliu@163.com; liufh@mail.sxu.cn

ergies. From the points of interacting mechanisms, all the heavy ion accelerators at different energies are needed for us because they can supply a deficiency and support an argument each other. The energy of 1—2 GeV/nucleon is at the low-energy end of high energies. It is highly important for us to study the processes of heavy ion collisions at 1—2 GeV/nucleon because some interacting mechanisms may be changed from the intermediate energy range to high one. To investigate heavy ion collisions at the low-energy end of high energies, the AGS was performed at a lower energy (2 GeV/nucleon<sup>[5]</sup>) due to the importance of this energy range. According to our guesses, the initial energy of nuclear limiting fragmentation may be lower than that of JINR/Nuclotron. It is one of our research directions to search the critical energy at which the interacting mechanisms and fragmentation modes had changed. The working energies of GSI/SIS and Lanzhou Cooling Storage Ring (CSR) are at 1—2 GeV/nucleon and lower. They give us a chance to study the heavy ion collisions at low and intermediate energies and at low-energy end of high energies.

To study the emissions of nuclear fragments and mesons produced in heavy ion collisions at low and intermediate energies and at low-energy end of high energies, we have suggested a MSIG model in our previous work<sup>[6–10]</sup> and described some experimental data. In this paper, we will use the MSIG model to study the emissions of nuclear fragments and mesons produced in heavy ion collisions at the CSR and related energies.

## 2 The MSIG model

The MSIG model<sup>[6–10]</sup> was suggested in the framework of Maxwell's ideal gas model, the latter one can be found in general textbook of thermodynamics. According to the MSIG model, many emission sources of fragments and particles are formed in heavy ion collisions at intermediate and high energies. In the rest frame of an emission source, the final-state products are assumed to emit isotropically. The momentum components in a right angle coordinate are assumed to obey Gaussian distribution. Interactions among different sources affect the momentum distributions of final-state products. Let the incident direction be  $oz$  axis and the reaction plane be  $xoz$  plane. Then, a right angle coordinate is built. In the coordi-

nate system,  $ox$  axis is exactly the direction of impact parameter. In the rest frame of an emission source, the components  $p'_x$ ,  $p'_y$ , and  $p'_z$  of momentum  $\mathbf{p}'$  are described by Gaussian distribution with a width  $\sigma$ . Considering the interactions among different sources, the source concerned by us will have an expansion and a movement in the momentum space. As a result, the momentum  $\mathbf{p}$  measured in final state will differ from  $\mathbf{p}'$ . The simplest relationship between  $\mathbf{p}$  and  $\mathbf{p}'$  is linear. We have component expressions as follows

$$p_{x,y,z} = a_{x,y,z}p'_{x,y,z} + B_{x,y,z} = a_{x,y,z}p'_{x,y,z} + b_{x,y,z}\sigma, \quad (1)$$

where  $B_{x,y,z}$  describe the movement of emission source and  $a_{x,y,z}$  and  $b_{x,y,z}$  denote the expansion and movement coefficients of the emission source respectively.

Eq. (1) is only an approximate expression for mean effect. It does not obey the Lorentz transition. The relativistic effect has not been considered in Eq. (1) because the energies concerned in the present work are not in a high-energy range. According to the knowledge of probability, the distributions of momentum components  $p_{x,y,z}$ , transverse momentum  $p_T$ , momentum  $p$ , azimuthal angle  $\varphi$ , and space angle  $\vartheta$  can be obtained. Using the Monte Carlo method, the corresponding distributions and correlations can be given in terms of random variables (see Refs. [11, 12] for details).

In the above discussions, the parameters  $a_x$ ,  $a_y$ ,  $b_x$ , and  $b_y$  describe the transverse structure of emission source in the momentum space.  $a_x > 1$  and  $a_y > 1$  mean expansions of the emission source along the directions of  $\pm x$  and  $\pm y$  respectively;  $b_x(b_y) > 0$  and  $b_x(b_y) < 0$  mean movements of the emission source along the directions of  $+x(+y)$  and  $-x(-y)$  respectively. An isotropic emission results  $a_{x,y} = 1$  and  $b_{x,y} = 0$ .

## 3 Comparison with other modelling results and experimental data

**Firstly**, we give a comparison with calculated results of IDQMD model at 25 MeV/nucleon. In the energy range of a few decades MeV, we have not found available experimental data. However, we may compare our calculated results with those of the IDQMD model<sup>[13]</sup>. We notice that the published IDQMD

modelling results are not compared with experimental data, too.

The interactions of  $^{86}\text{Kr}$ - $^{124}\text{Sn}$  with impact parameter  $b=7$ – $10$  fm at incident energy 25 MeV/nucleon have been investigated by us. The distributions  $AdN/dp_x$ ,  $A^2dN/p_T dp_T$ , and  $kdN/d\varphi$  are obtained for light fragments (with mass number  $A=1$ – $4$ ), where  $N$  denotes the number of fragments and  $k$  is used to keep the mean value of  $kdN/d\varphi$  to be 1. Meanwhile, the correlations between the elliptic flow [ $v_2 = \langle \cos(2\varphi) \rangle$ ] per nucleon  $v_2/A$  and  $p_T/A$ , as well as the fourth-order anisotropic flow [ $v_4 = \langle \cos(4\varphi) \rangle$ ] per nucleon  $v_4/A$  and  $p_T/A$  are studied, where  $\langle \dots \rangle$  denotes an average over the fragments concerned.

Comparing with the calculated results of the IDQMD model<sup>[13]</sup>, we found that our calculated distribution of transverse momenta is approximately in agreement with that of the IDQMD model. Our calculated distributions of momentum components and azimuthal angles are in good agreement with those of the IDQMD model respectively. The correlations between  $v_2/A$  and  $p_T/A$ , as well as  $v_4/A$  and  $p_T/A$ , calculated by us are qualitatively in agreement with those of the IDQMD model respectively. The main results discussed in the first part has been published elsewhere<sup>[11]</sup>.

**Secondly**, we show a comparison with experimental data in an energy range of hundreds MeV/nucleon. The experimental results show that multiplicity distributions in heavy ion collisions at different incident energies display a uniform shape. Generally, the distribution curve decreases monotonously with increasing of the multiplicity, and a plateau structure appears in the middle multiplicity; then the distribution curve falls rapidly, and a knee structure appears in the tail part of high multiplicity. For convenience in the description of this part, we divide particle multiplicity into a few bins. According to Ref. [14], for the multiplicity distribution of protons, the multiplicity corresponding to a half highness of the plateau is denoted by  $N_p^{\text{max}}$ . From 0 to  $N_p^{\text{max}}$  the multiplicities are divided into four bins, i.e. MUL1= $(0-0.25)N_p^{\text{max}}$ , MUL2= $(0.25-0.5)N_p^{\text{max}}$ , MUL3= $(0.5-0.75)N_p^{\text{max}}$ , and MUL4= $(0.75-1)N_p^{\text{max}}$ . In addition, the fifth bin MUL5 is in the range from  $N_p^{\text{max}}$  to maximum multiplicity.

The azimuthal distributions,  $kdN/d\varphi$ , of final-

state fragments produced in the third multiplicity bin MUL3 in Au-Au collisions at 150, 200, 250, 400, 650, and 800 MeV/nucleon are given in Fig. 1. The histograms are the experimental data of Ref. [14], and the solid curves are our calculated results. In the calculation, the parameter values obtained by fitting the experimental data are marked in the figure. One can see that the calculated results of our MSIG model are in agreement with the experimental data.

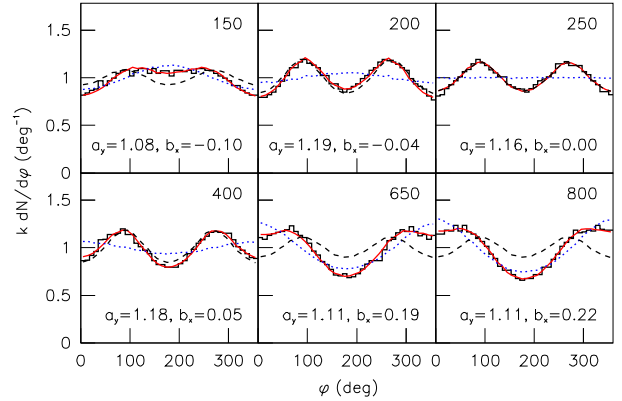


Fig. 1. Azimuthal distributions of fragments, for the multiplicity bin MUL3, produced in Au-Au collisions at the indicated beam energies in MeV/nucleon. The histograms are the experimental data of Ref. [14]. The solid curves are our calculated results with the parameter values indicated in the figure. The dashed and dotted curves are the contributions of the sources expansion and movement respectively.

Similarly, the azimuthal distributions of final-state fragments produced in the multiplicity bins MUL1-MUL5 in Ca-Ca, Nb-Nb, and Au-Au collisions at 400 MeV/nucleon are shown in Fig. 2. In Fig. 3, the azimuthal distributions of final-state protons, helium, and all fragments produced in Au-Au collisions at 400 MeV/nucleon are presented, where the right panel is the same as that in Fig. 2. Once more our calculated results describe the experimental data.

To see the dependence of the calculated results on the parameter values, the calculated results in the case of keeping  $a_x(a_y)$  not to be changed and letting  $b_x(b_y) = 0$  are given in Figs. 1–3 by the dashed curves; and the calculated results in the case of keeping  $b_x(b_y)$  not to be changed and letting  $a_x(a_y) = 1$  are given in Figs. 1–3 by the dotted curves. The results corresponding to  $b_x(b_y) = 0$  are the contributions of source expansion effects; and the results corresponding to  $a_x(a_y) = 1$  are the contributions of source movement effects.

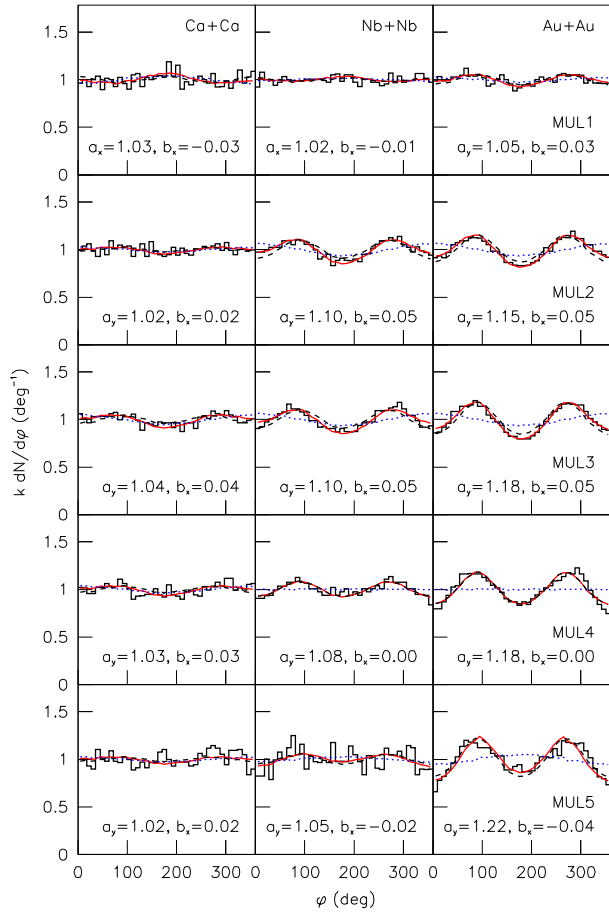


Fig. 2. As for Fig. 1, but showing the results of fragments produced in Ca-Ca, Nb-Nb, and Au-Au collisions at 400 MeV/nucleon.

**Thirdly**, we present a comparison with experimental data at 1–2 GeV/nucleon. In the above two parts, the  $ox$  axis is defined by the impact parameter. In the case of defining the impact parameter as the  $oy$  axis, the situation is similar. In fact, two definitions are used in the references. Differing from the above parts, the latter definition is used in this part. Both the coordinating systems have the same  $oz$  axis.

In the above two parts, we have discussed collisions at low and intermediate energies. The final-state products in these collisions are mainly nuclear fragments. In the third part, we focus our attention on collisions at the low-energy end of high energies. Some pions and kaons will be produced in these collisions.

The azimuthal distributions of  $\pi^+$  and  $K^+$  produced in Au-Au collisions at 1.5 GeV/nucleon,  $\pi^+$ ,  $K^+$ , and  $K^-$  produced in Ni-Ni collisions at 1.93 GeV/nucleon, and  $\pi^+$  and  $K^+$  produced in Au-Au collisions at 1 GeV/nucleon have been investigated by us. Meanwhile, the emission angular dis-

tributions of  $K^+$  and  $K^-$  produced in Au-Au collisions at 1.5 GeV/nucleon and in Ni-Ni collisions at 1.93 GeV/nucleon with other cut condition are calculated. Our calculated results show that the MSIG model describes the experimental data reported in Refs. [15–19]. The main results discussed in the third part has been published elsewhere<sup>[12]</sup>.

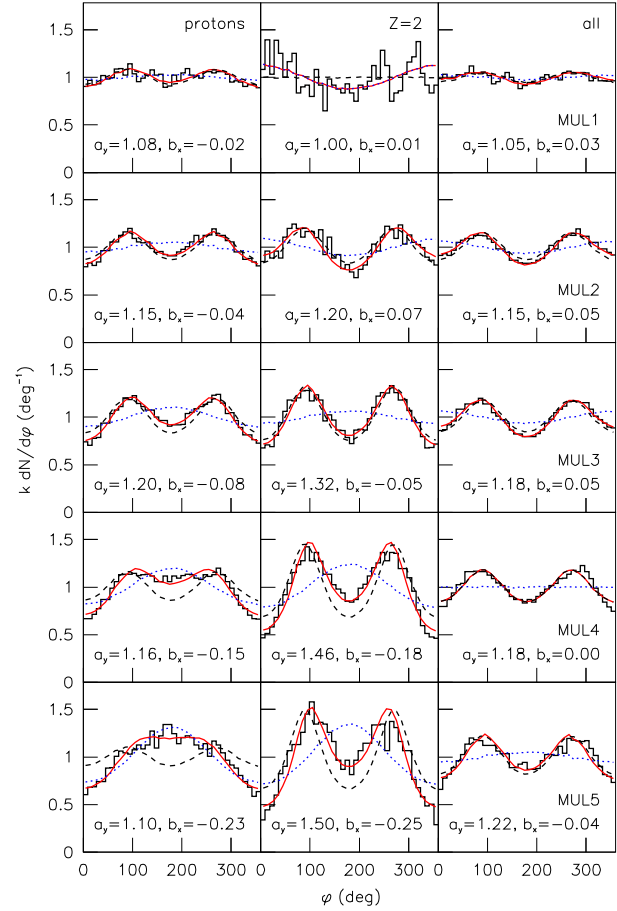


Fig. 3. As for Fig. 1, but showing the results of protons, fragments with  $Z = 2$ , and all fragments produced in Au-Au collisions at 400 MeV/nucleon.

## 4 Conclusions

Three contents have been studied in the present work. Firstly, we have compared the calculated results of the MSIG and IDQMD models at a few decades MeV/nucleon. It is found that the two distributions of transverse momentums are qualitatively in agreement with each other. The two distributions of momentum components and the two distributions of azimuthal angles are respectively in good agreement with each other. The dependence of elliptic flow on transverse momentum and the depen-

dence of the fourth-order anisotropic flow on transverse momentum calculated by the MSIG model describe approximately the corresponding results of the IDQMD model<sup>[13]</sup>. Secondly, the calculated results of the MSIG model are compared and found to be in agreement with the experimental azimuthal distributions of nuclear fragments produced in heavy ion collisions<sup>[14]</sup> in hundreds MeV/nucleon energy range. Finally, the calculated results of the MSIG model are compared and found to be in agreement with the experimental azimuthal and angular distributions of pions and kaons produced in heavy ion collisions<sup>[15–19]</sup>

at the low-energy end of high energies.

The parameters  $a$ ,  $b$ , and  $\sigma$  describe respectively the expansion coefficient, movement coefficient, and excitation degree of emission source. The expansion coefficient  $a > 1$  and  $a = 1$  denote that the emission source has an expansion and no expansion respectively. The physics condition requests that  $a \geq 1$ . The movement coefficient  $b > 0$ ,  $b < 0$ , and  $b = 0$  denote that the emission source has a movement along the positive direction of coordinate axis, a movement along the negative direction of coordinate axis, and no movement, respectively.

---

## References

- 1 Hwa R C. Quark-Gluon Plasma. Singapore: World Scientific, 1990. 1
- 2 Back B B et al. Phys. Rev. C, 2002, **66**: 054901
- 3 Bearden et al. Phys. Rev. Lett., 2002, **88**: 202301
- 4 <http://lhc.web.cern.ch/lhc/>
- 5 Klay J L et al. Phys. Rev. Lett., 2002, **88**: 102301
- 6 LIU Fu-Hu. Europhys. Lett., 2003, **63**: 193
- 7 LIU Fu-Hu et al. Int. J. Mod. Phys. E, 2003, **12**: 713
- 8 LIU Fu-Hu, Abd Allah N N, Singh B K. Phys. Rev. C, 2004, **69**: 057601
- 9 LIU Fu-Hu. Can. J. Phys., 2004, **82**: 109
- 10 LIU Fu-Hu et al. Chin. J. Phys., 2004, **42**: 152
- 11 LIU Fu-Hu, LI Jun-Sheng, DUAN Mai-Ying. Phys. Rev. C, 2007, **75**: 054613
- 12 LIU Fu-Hu. Chin. Phys. B, 2008, **17**: 883
- 13 YAN T Z et al. Phys. Lett. B, 2006, **638**: 50
- 14 Gutbrod et al. Phys. Rev. C, 1990, **42**: 640
- 15 Uhlig F et al. Phys. Rev. Lett., 2005, **95**: 012301
- 16 Forster A for the KaoS Collaboration. J. Phys. G, 2005, **31**: S693
- 17 Brill D et al. Phys. Rev. Lett., 1993, **71**: 336
- 18 Shin Y et al. Phys. Rev. Lett., 1998, **81**: 1576
- 19 Menzel M et al. Phys. Lett. B, 2000, **495**: 26